



Contents lists available at [SciVerse ScienceDirect](http://SciVerse.ScienceDirect.com)

European Journal of Cell Biology

journal homepage: www.elsevier.de/ejcb



NG2-mediated Rho activation promotes amoeboid invasiveness of cancer cells

Daniela Paňková^a, Njainday Jobe^a, Magdalena Kratochvílová^a, Roberto Buccione^b, Jan Brábek^a, Daniel Rösel^{a,*}

^a Department of Cell Biology, Faculty of Science, Charles University in Prague, Vinicna 7, 128 43 Prague 2, Czech Republic

^b Tumour Cell Invasion Laboratory, Consorzio Mario Negri Sud, S. Maria Imbaro, Chieti 66030, Italy

ARTICLE INFO

Article history:

Received 14 February 2012

Received in revised form 2 May 2012

Accepted 3 May 2012

Keywords:

NG2

Invasiveness

Amoeboid

Mesenchymal

Rho

Invadopodia

ABSTRACT

The aim of this study was to analyze the potential role of NG2 chondroitin sulfate proteoglycan in amoeboid morphology and invasiveness of cancer cells. In the highly metastatic amoeboid cell lines A3 and A375M2, siRNA-mediated down-regulation of NG2 induced an amoeboid-mesenchymal transition associated with decreased invasiveness in 3D collagen and inactivation of the GTPase Rho. Conversely, the expression of NG2 in mesenchymal sarcoma K2 cells as well as in A375M2 cells resulted in an enhanced amoeboid phenotype associated with increased invasiveness and elevated Rho-GTP levels. Remarkably, the amoeboid-mesenchymal transition in A375M2 cells triggered by NG2 down-regulation was associated with increased extracellular matrix-degrading ability, although this was not sufficient to compensate for the decreased invasive capability caused by down-regulated Rho/ROCK signaling. Conversely, in K2 cells with overexpression of NG2, the ability to degrade the extracellular matrix was greatly reduced. Taken together, we suggest that NG2-mediated activation of Rho leading to effective amoeboid invasiveness is a possible mechanism through which NG2 could contribute to tumor cell invasion and metastasis.

© 2012 Elsevier GmbH. All rights reserved.

Introduction

The main cause of mortality by cancer is due to the ability of tumor cells to spread to distant locations in the body and thereby form metastases. The process starts with local invasion to adjacent tissue, which is a key determinant of the metastatic potential. Tumor cells invade either collectively, retaining their intracellular junctions, or individually (reviewed in Panková et al., 2010). Individual cell migration is broadly classified as either mesenchymal or amoeboid (reviewed in Panková et al., 2010; Friedl, 2004; Lämmermann and Sixt, 2009).

Cells with mesenchymal morphology exhibit, in a 3D environment, an elongated spindle-like morphology with one or more leading pseudopodia. Their movement is initiated by the formation of actin rich filopodia and lamellipodia. This process is controlled by the small Rho-GTPases Rac and Cdc42 (Sahai and Marshall, 2003; Sanz-Moreno et al., 2008). To invade the extracellular matrix (ECM), mesenchymal cells in vitro employ specified cellular structures called invadopodia; motile cellular protrusions with an ability to invade the surrounding ECM via its degradation (Caldieri et al., 2009; Tolde et al., 2010).

Cells with amoeboid-like type migration exhibit a round shape in 3D environments. Their movement is characterized by cycles of expansion and contraction of the cell body and bleb like protrusions mediated by cortically localized acto-myosin interactions (Wolf et al., 2003; Sahai and Marshall, 2003). This process is promoted by the up-regulation of Rho/ROCK signaling. The increased Rho/ROCK signaling has been shown to assist in the generation of sufficient acto-myosin forces allowing the amoeboid tumor cells to push through the extracellular matrix independently of the extracellular matrix degradation (Rosel et al., 2008).

Amoeboid and mesenchymal invasion modes are not mutually exclusive. Suppression or enhancement of specific molecular pathways can induce a mesenchymal-amoeboid transition or amoeboid-mesenchymal transition (reviewed in Panková et al., 2010). Invasion by both types of cells requires adhesion to components of the ECM and acto-myosin contraction to promote migration. The adhesion of mesenchymal cells is mainly mediated via integrins; but amoeboid cells typically express integrins at very low levels (Rosel et al., 2008). The low expression of integrins in amoeboid cells is apparently at odds with their increased ability to generate traction forces. It was recently suggested, however, that amoeboid cell adhesion to the ECM can be mediated by non-integrin receptors such as glycoproteins (Friedl, 2004).

NG2 chondroitin sulfate proteoglycan (a.k.a. CSPG-4, MCSP) is an integral membrane proteoglycan found on the surface of many different types of progenitor cells (Nishiyama et al., 1991). NG2

* Corresponding author. Tel.: +420 22195 1769; fax: +420 22195 1761.
E-mail address: rosel@natur.cuni.cz (D. Rösel).

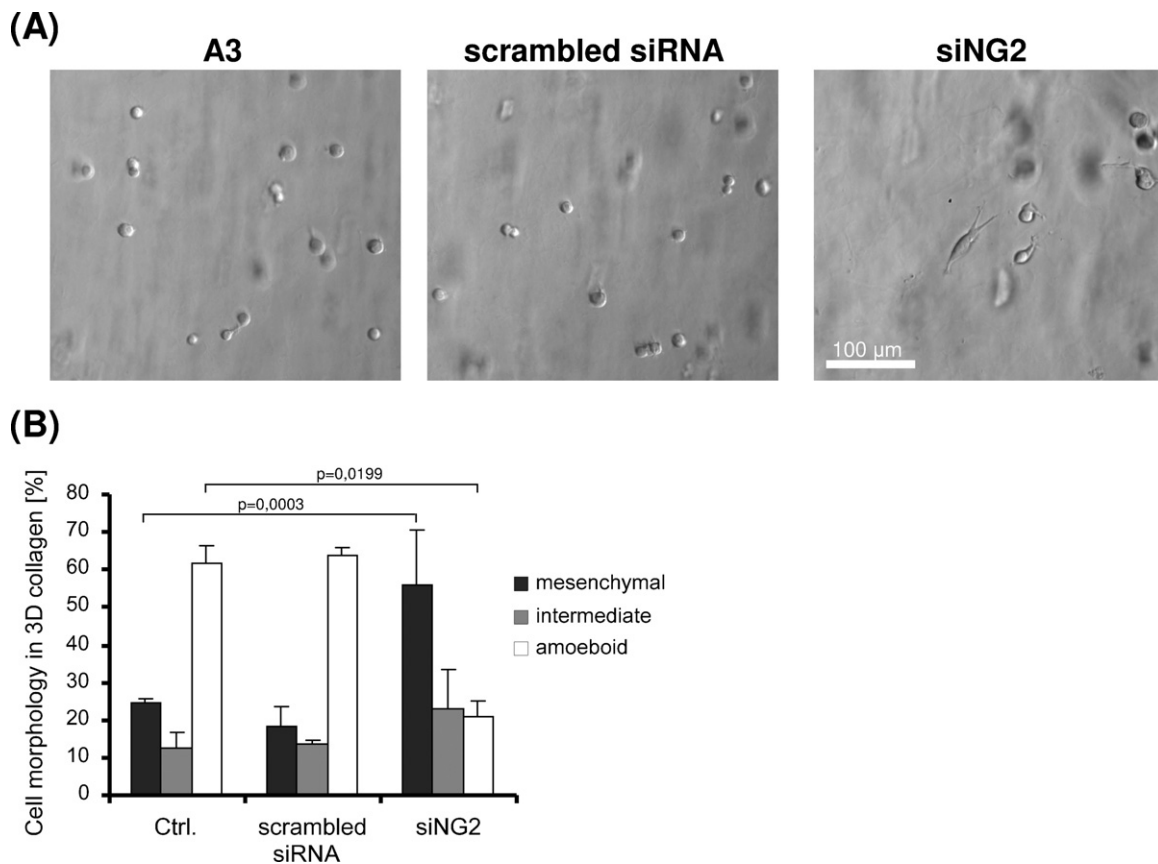


Fig. 1. Effect of NG2 silencing on morphology of A3 sarcoma cells. (A) Cells were grown in 3D collagen and after 24 h cell morphology was analyzed and documented using photomicroscopy. Left panel: A3 cells; medium panel: A3 cells treated with scrambled siRNA; right panel: A3 cells treated with NG2-specific siRNA. (B) Quantitative analysis of the cell morphology. Cells were grown in 3D collagen and after 24 h the morphology of cells was analyzed using photomicroscopy and classified on the basis of the elongation index as described in section “Materials and methods”.

was shown to mediate adhesion of cells to collagen and other ECM components (Stallcup et al., 1990; Burg et al., 1996; Tillet et al., 1997). Here we show that NG2 expression has pro-amoeboid effects on tumor cells, whereas its inhibition appears pro-mesenchymal. Our results further suggest that NG2 affects tumor cell behavior through the regulation of Rho. The pro-amoeboid effects of NG2 together with its ability to bind components of ECM suggest that NG2 could be a non-integrin ECM receptor of amoeboid cells.

Materials and methods

Cells and culture

K2 cells, full name LW13K2, are spontaneously transformed rat embryonic fibroblasts. The A3 cells, full name A337/311RP, were developed from K2 by neoplastic progression in vivo and in vitro (Cavanna et al., 2007, PMID: 17264155). K2 and A3 cells were cultivated in MEM with Hanks’ salts (HMEM) supplemented with 10% bovine serum (ZVOS), 0.09% sodium bicarbonate, 0.12 g/l sodium pyruvate, and 1 mmol/l glutamine at 37 °C with 5% CO₂. A375M2 melanoma cells (obtained from Prof. R. Hynes) were routinely maintained in DMEM (GIBCO) with 4500 mg/l L-glucose, L-glutamine, and pyruvate, supplemented with 10% fetal bovine serum (Sigma), 2% antibiotic–antimycotic (GIBCO) and 1% MEM non-essential amino acids (GIBCO).

siRNA and cDNA transfection

A375M2, A3 and K2 cells were plated at 60% confluence on 6-well plates and after 24 h transfected with 60 pmol of siRNA using LipofectamineRNAiMax (Life Technologies) for A3 and K2 cells, or jet Prime DNA and siRNA transfection reagent (Polyplus) for A375M2 cells. SiRNAs against human (A375M2) and rat (A3, K2 cells) NG2 were purchased from Life Technologies. For siRNA rescue experiments, the transfection mixture was further supplemented with 5 μ g of rat *ng2* cDNA plasmid – kind gift from Prof. W. Stallcup (Sanford-Burnham Medical Research Institute, Cancer Center, La Jolla, CA). Knockdown and reexpression of NG2 was confirmed by flow cytometry. In preliminary testing three siRNA oligos were used. In all cases the successful knockdown of NG2 led to amoeboid-mesenchymal transition. For further experiments only the most effective oligo was chosen.

To achieve stable transfection of K2 cells, the NG2 cDNA was first recloned using BamHI/NotI to pIRESpuro3 vector (Invitrogen) and K2 cells were transfected with the resulting construct. Transfected K2 cells were then selected with 7 μ g/ml puromycin for 4 weeks after which time individual colonies were isolated, and NG2 overexpression was confirmed by flow cytometry.

Immunoblotting and Rho pull-down assays

Confluent cell cultures were washed with phosphate buffered saline (PBS) and lysed in modified RIPA buffer (50 mM Tris-HCl (pH 7.4), 150 mM NaCl, 5 mM EDTA, 1% NP40, 1% sodium deoxycholate,

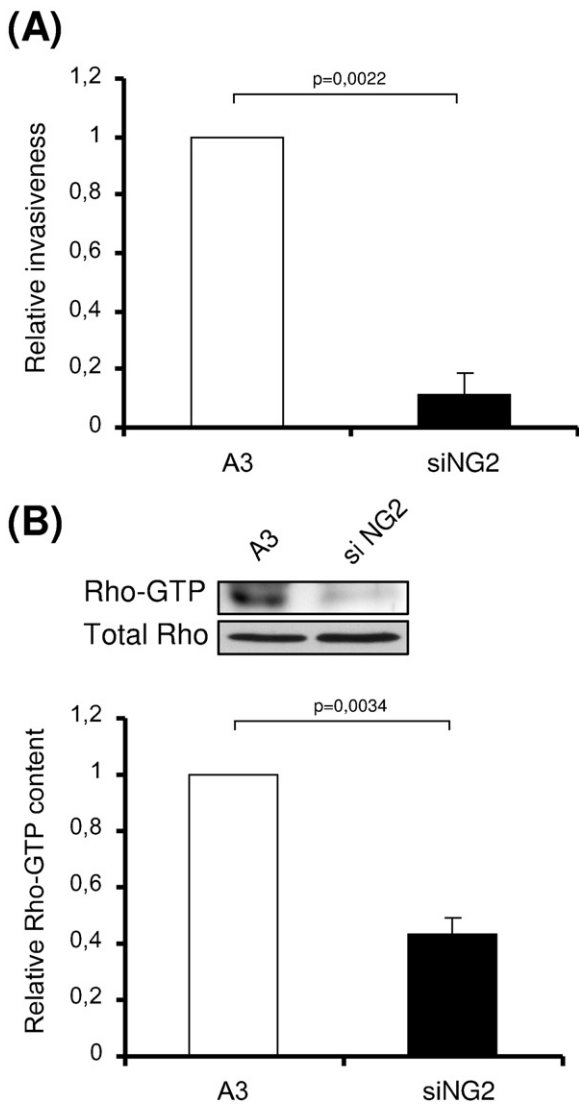


Fig. 2. Effect of NG2 silencing on invasiveness and Rho-GTP levels in A3 sarcoma cells. (A) 3D collagen invasion assay. Cells were seeded on top of a collagen gel and their invasion was scored as described in section “Materials and methods”. Bars represent the mean invasion depth, normalized to that of untreated A3 cells. (B) Cell lysates of each cell variant were prepared, and total GTP-bound Rho was enriched by absorbing cell lysates to GST-RBD beads and measured by Western blotting using pan-Rho antibody. Densitometric ratios of total Rho and Rho-GTP signal were determined and normalized to that of untreated A3 cells. The error bars represents standard deviations and p values indicate statistical significances. Representative immunoblots of total (left) and GTP-loaded (right) Rho are shown.

50 mM NaF, 1% aprotinin and 0.1 mM Na₃VO₄). Protein concentrations in lysates were determined using the BCA assay (Pierce). For immunoblotting, samples were separated on 12% SDS-polyacrylamide gels and transferred onto nitrocellulose membranes. Non-specific activity was blocked by incubating 45 min at room temperature in Tris-buffered saline containing 0.05% Tween-20 (TBST) and 4% bovine serum albumin (BSA). Membranes were then incubated overnight in primary antibody, washed extensively with TBST, and then incubated for 1 h at room temperature with HRP-conjugated secondary antibody. After extensive washing in TBST, the blots were developed by enhanced chemiluminescence and exposed by using LAS 4000 Luminiscent image reader (Fuji-film Life Sciences). RhoA pull-down assays were performed using by GST-rhotekin and Rho pull-down detection kit according to the manufacturer’s instructions (Thermo Scientific). The levels of total and active RhoA were revealed using a Rho-specific antibody.

Antibodies against NG2 and HRP-conjugated anti-mouse and anti-rabbit secondary antibodies were obtained from Santa Cruz Biotechnology Inc. Anti-pY421 Cortactin, Alexa Fluor 594-phalloidin, anti-rabbit (Alexa Fluor-594) and anti-mouse (Alexa Fluor-488) were from Life Technologies. Antibody against Rho was from Thermo Scientific (Pierce Biotechnology, USA).

Cell invasion and morphology assays in 3D collagen

The 3D collagen invasion assay was performed as described previously (Janostiak et al., 2011). Briefly, a 200 μl solution containing 2 mg/ml Collagen R (Serva) and 4 mg/ml collagen G (Biochrom) was prepared, and 46 μl of NaHCO₃ and 46 μl HMEM were added. 10 μl of the collagen solution was added into each well of μ-Slide Angiogenesis plate and polymerized at 37 °C. 50 μl of cell suspension (2 × 10⁵ cells/ml) was added on top of a collagen gel. After 2 days, invasion was scored as an average invasion depth of the cells in selected field of view using Nikon-Eclipse TE2000-S (20×/0.40 HMC objective) and NIS-Elements software. For each experiment, 10 μm optical sections were analyzed in 6 fields of view. In order to compare between individual experiments, average invasion depth was normalized to that of untreated cells.

To analyze cell morphology in 3D collagen, cells were trypsinized, washed in complete medium, counted and 10⁵ cells were mixed with 500 μl of 3 mg/ml Collagen R in complete medium. The suspension of cells in collagen (500 μl) was loaded to a well in a 12-well plate, the gel was allowed to polymerize at 37 °C for 30 min and overlaid with complete medium. After 24 h the morphology of cells in 3D collagen was analyzed using Nikon Eclipse TE2000-S microscope (20×/0.40 HMC objective). Cell morphology was classified on the basis of the elongation index. The elongation index was calculated as the length divided by the width. Cells whose elongation index was more than 3 were considered mesenchymal. Intermediate cells had an elongation index of 2–3; for amoeboid cells, the index was 1–2. Dividing cells were excluded from the analysis. For each condition a minimum of 300 cells per experiment were analyzed for morphology in 3D collagen.

Gelatin degradation assay

Dry coverslips were coated with a thin layer of FITC-conjugated gelatin and immediately overturned on a drop of 0.5% ice-cold glutaraldehyde in PBS for 15 min incubation in the dark. Coverslips were then transferred to a 12-well plate, with the coated side up and gently washed three times with PBS, incubated with sodium borohydride (5 mg/ml) in PBS for 3 min and then finally washed with PBS. The cover slips were sterilized in 70% ethanol for 1 min, dried for 10 min in a sterile hood and quenched in complete medium for 1 h at 37 C. 3 × 10⁴ cells were plated on fluorescent gelatin-coated coverslips in media containing 10 μM Batimastat (Tocris Biosciences, UK) and allowed to adhere at 37 °C overnight. Cells were washed three times with medium to remove the inhibitor and incubated another 3 h in complete medium. After 3 h, the coverslips were washed, fixed in 4% paraformaldehyde and permeabilized with 0.1% Triton X-100 in PBS for 15 min. After blocking for 30 min in 5% BSA, F-actin was stained with Alexa594-conjugated phalloidin. Coverslips were mounted using Mowiol reagent and representative fields were documented by photomicroscopy using a Nikon Eclipse TE2000-S microscope (20×/0.75 Plan Apo objective) mounted with VDS Vosskühler CCD-1300 camera. To quantify areas of degradation, for each independent experiment we considered 10 random fields. The value of each degradation area was measured using the public domain software Imagej; the total area degraded in the captured field was then normalized for the number of cells (Ayala et al., 2008). The effect of each treatment was expressed as

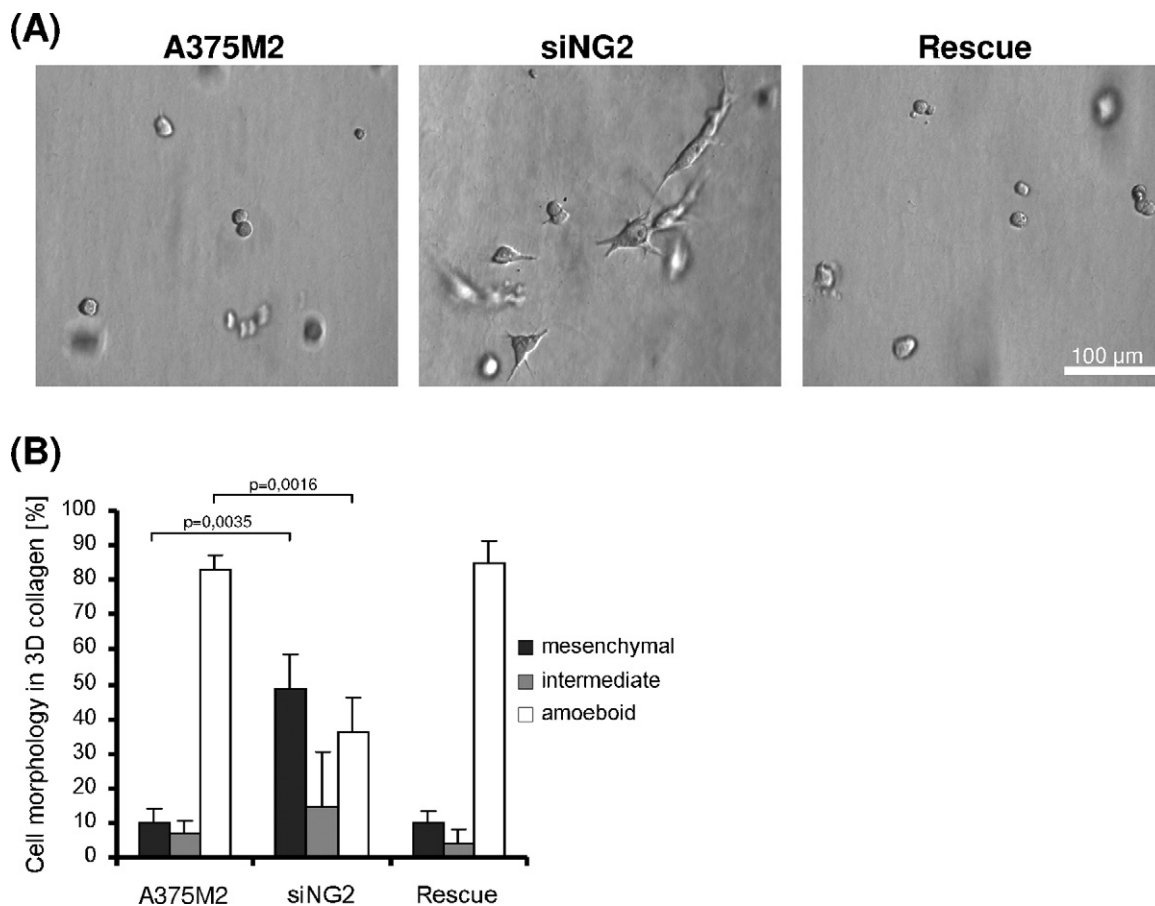


Fig. 3. Effect of NG2 silencing on morphology of A375M2 melanoma cells. (A) Cells were grown in 3D collagen and after 24 h cell morphology was analyzed and documented using photomicroscopy. Left panel: A375M2 cells; medium panel: A375M2 cells treated with NG2-specific siRNA; right panel: A375M2 cells treated with NG2-specific siRNA and rat NG2 cDNA (rescue). (B) Quantitative analysis of cell morphology. Cells were grown in 3D collagen and after 24 h cell morphology was analyzed using photomicroscopy and classified on the basis of the elongation index as described in section “Materials and methods”.

relative degradation: degradation normalized to control untreated cells.

Flow cytometry

Confluent cells were harvested, washed twice in ice cold FACS buffer (HBSS buffer supplemented with 20 mM glucose, 2% fetal bovine serum (Sigma), 2% antibiotic–antimycotic (GIBCO)), resuspended at 10^7 /ml in FACS buffer, and 10^6 cells were incubated with anti-NG2 antibody. After 30 min at 4°C, cells were washed and stained in dark for 20 min with Alexa Fluor-488 conjugated goat anti-mouse antibody. Flow cytometry was performed using a BD FACS Vantage SE system (BD Biosciences).

Statistical analysis

Statistical significances were determined using an unpaired, two tailed, Student’s *t* test.

Results

To analyze the potential role of NG2 in amoeboid invasiveness, we employed a fibrosarcoma-derived cell model consisting of highly invasive and metastatic A3 cells and the parental, non-invasive K2 counterparts (Cavanna et al., 2007). The A3 cells adopt, in a 3D environment, amoeboid morphology and invasiveness, while K2 cells possess a mesenchymal morphology (Rosel et al., 2008). Previously reported expression microarray analysis of A3

and K2 cells revealed that *ng2* mRNA is 65-fold overexpressed in A3 cells (Cavanna et al., 2007). NG2 is a chondroitin sulfate proteoglycan which can mediate cell adhesion to collagen and other ECM components in an integrin-independent manner (Tillet et al., 2002), and could thus represent the non-integrin ECM receptor of amoeboid cells. At the protein level, we confirmed high expression of NG2 in A3 cells, while expression in K2 cells was below detection (Supplementary Fig. 1).

To analyze the potential role of NG2 in amoeboid invasiveness, we performed siRNA-mediated knock down of NG2 in A3 cells. We found that NG2 knock down lead to an amoeboid-mesenchymal transition; the number of amoeboid cells was decreased more than 2 fold and, simultaneously, the number of cells with mesenchymal morphology proportionally increased (Fig. 1, Supplementary Fig. 2). Next, we analyzed the effect of NG2 silencing on invasiveness in 3D collagen. We found that siRNA-mediated knockdown of NG2 resulted in a profound (more than 9-fold) decrease of the ability of cells to invade a 3D collagen gel (Fig. 2A). Amoeboid invasiveness of A3 cells is mediated through the Rho/ROCK pathway and is accompanied by elevated levels of Rho-GTP (Rosel et al., 2008). To determine whether the decreased capability of NG2-silenced A3 cells is associated with inhibition of Rho, we performed a Rho-activation assay. Consistent with decreased invasiveness, NG2-silenced A3 cells exhibited greatly decreased Rho-GTP levels (Fig. 2B).

To further confirm the effect of NG2 on amoeboid morphology and invasiveness in an independent model, we employed A375M2 melanoma cells, which preferentially exhibit amoeboid

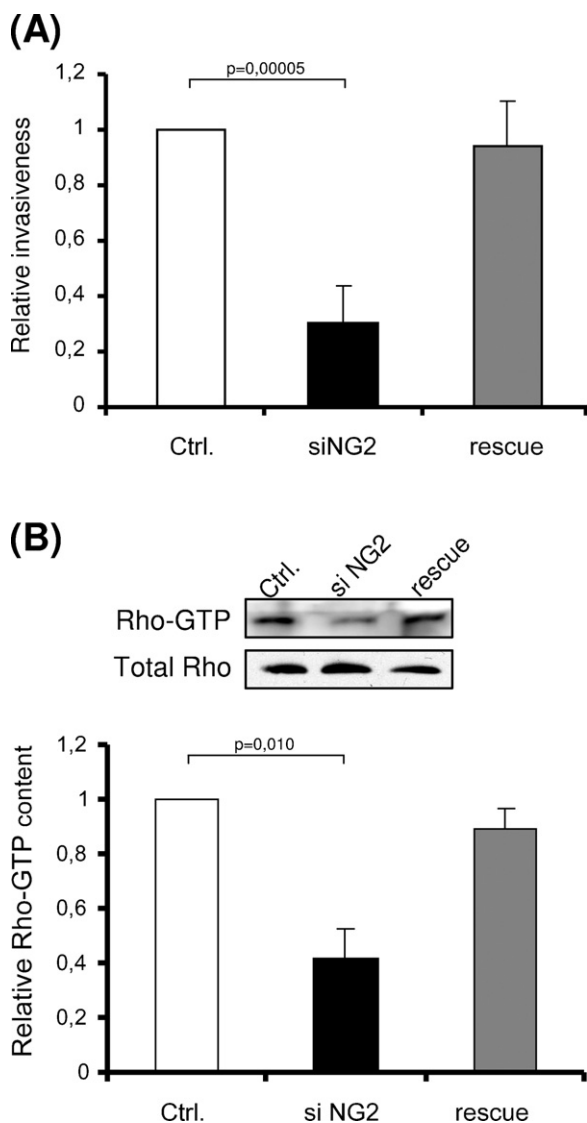


Fig. 4. Effect of NG2 silencing on invasiveness and Rho-GTP levels in A375M2 melanoma cells. (A) 3D collagen invasion assay. Cells were seeded on top of a collagen gel and their invasion was scored as described in section “Materials and methods”. Bars represent the mean invasion depth, normalized to that of untreated A375M2 cells. (B) Cell lysates of each cell variant were prepared, and total GTP-bound Rho was enriched by absorbing cell lysates to GST-RBD beads and measured by Western blotting using pan-Rho antibody. Densitometric ratios of total Rho and Rho-GTP signal were determined and normalized to that of untreated A375M2 cells. The error bars represent standard deviations and p values indicate statistical significances. Representative immunoblots of total (left) and GTP-loaded (right) Rho are shown.

morphology in 3D collagen (Pinner and Sahai, 2008). Unlike A3 fibrosarcoma cells, the A375M2 cells, although amoeboid in 3D collagen, retained the ability to form invadopodia and degrade the ECM (Wolf et al., 2003; Buccione et al., 2005). The NG2 expression in A375M2 cells is approximately 8 times lower than in A3 cells (Supplementary Fig. 3). Nevertheless, similar to A3 cells, siRNA mediated silencing of NG2 resulted in amoeboid-transition, manifested by more than 2 fold decrease in number of amoeboid cells (Fig. 3, Supplementary Fig. 4). Re-expression of non-targeted rat *ng2* cDNA in NG2-silenced A375M2 cells resulted in reversion of the amoeboid phenotype (Fig. 3, Supplementary Fig. 4). Next, we analyzed the effect of NG2 silencing on invasiveness. Consistent with results obtained in A3 cells, siRNA-mediated knockdown of NG2 in A375M2 cells resulted in a considerable (more than 3-fold) decrease of invasiveness (Fig. 4A) and again, the re-expression of

NG2 rescued invasiveness, almost to the level of control cells. To determine whether the effect of NG2 levels on invasiveness was associated with changes in Rho-GTP levels, we performed a Rho-activation assay. We found that while siRNA-mediated knockdown of NG2 in A375M2 cells results in a great decrease of Rho-GTP levels, re-introduction of NG2 increased Rho-GTP levels almost to the level found in control A375M2 cells (Fig. 4B).

Though predominantly amoeboid, A375M2 cells are capable of forming invadopodia (Baldassarre et al., 2003). We investigated whether the NG2-mediated effect on the ratio of amoeboid/mesenchymal cells correlated with effects on invadopodia activity. A gelatin degradation assay was performed with control and NG2-silenced A375M2 cells in the absence or presence of non-targeted rat NG2 cDNA re-expression. Remarkably, we found that siRNA mediated knockdown in A375M2 cells is associated with profound up-regulation of matrix-degrading activity, manifested by 19 fold increase in relative gelatin degradation (Fig. 5). This effect was reversed by re-expression of non-targeted rat *ng2* cDNA (Fig. 5).

Finally, we wondered whether the expression of NG2 in a predominantly mesenchymal cell line would be in itself sufficient to induce amoeboid morphology and increased invasiveness. For these experiments, we employed K2 cells (Cavanna et al., 2007). K2 cells, unlike A3, preferentially exhibit a mesenchymal morphology in a 3D environment and can degrade gelatin (Rosel et al., 2008). We analyzed the effect of NG2 overexpression in K2 cells, on morphology, invasiveness, Rho-GTPase levels and matrix degradation. Overexpression of NG2 in K2 cells resulted in a mesenchymal-amoeboid transition; the number of mesenchymal cells was decreased more than 2 fold and, simultaneously, the number of cells with amoeboid morphology has proportionally increased (Fig. 6A and B, Supplementary Fig. 5). The effect of NG2 overexpression on the morphology of K2 cells was efficiently blocked by incubation of the cells with ROCK inhibitor Y27632 (Fig. 6A and B). This further confirmed the dependence of NG2-induced mesenchymal-amoeboid transition on Rho/ROCK signaling. In addition, the mesenchymal-amoeboid transition induced by NG2 overexpression was accompanied by increased invasiveness and higher levels of activated Rho (Fig. 6C and D). Notably, the gelatin degradation assay showed a remarkable, 20-fold, decrease of matrix-degrading activity in K2 cells over-expressing NG2 (Fig. 7).

Taken together, these results suggest that NG2 glycoprotein is important for amoeboid morphology and invasiveness of cancer cells, and this effect is associated with increased Rho-GTP levels. In addition, NG2 expression has a strong negative regulatory effect on matrix-degrading activity.

Discussion

The aim of this study was to analyze the potential role of the NG2 chondroitin sulfate proteoglycan in cancer cell morphology and invasiveness. As a marker of poorly differentiated cells, NG2 has been implicated in human cancer progression. The human homologue of NG2 is expressed in most human melanomas. The expression of NG2 was found to enhance the growth and metastatic properties of melanoma cells (Burg et al., 1998). NG2 expression was also correlated with metastasis formation in soft-tissue sarcoma patients (Benassi et al., 2009). The correlation is so strong that NG2 expression can be used as a single predictive marker for metastasis progression in soft-tissue sarcomas. NG2 expression was also associated with progression of glioma (Stallcup and Huang, 2008), astrocytoma (Chekenya et al., 1999) and myeloid leukemia (Behm et al., 1996; Smith et al., 1996).

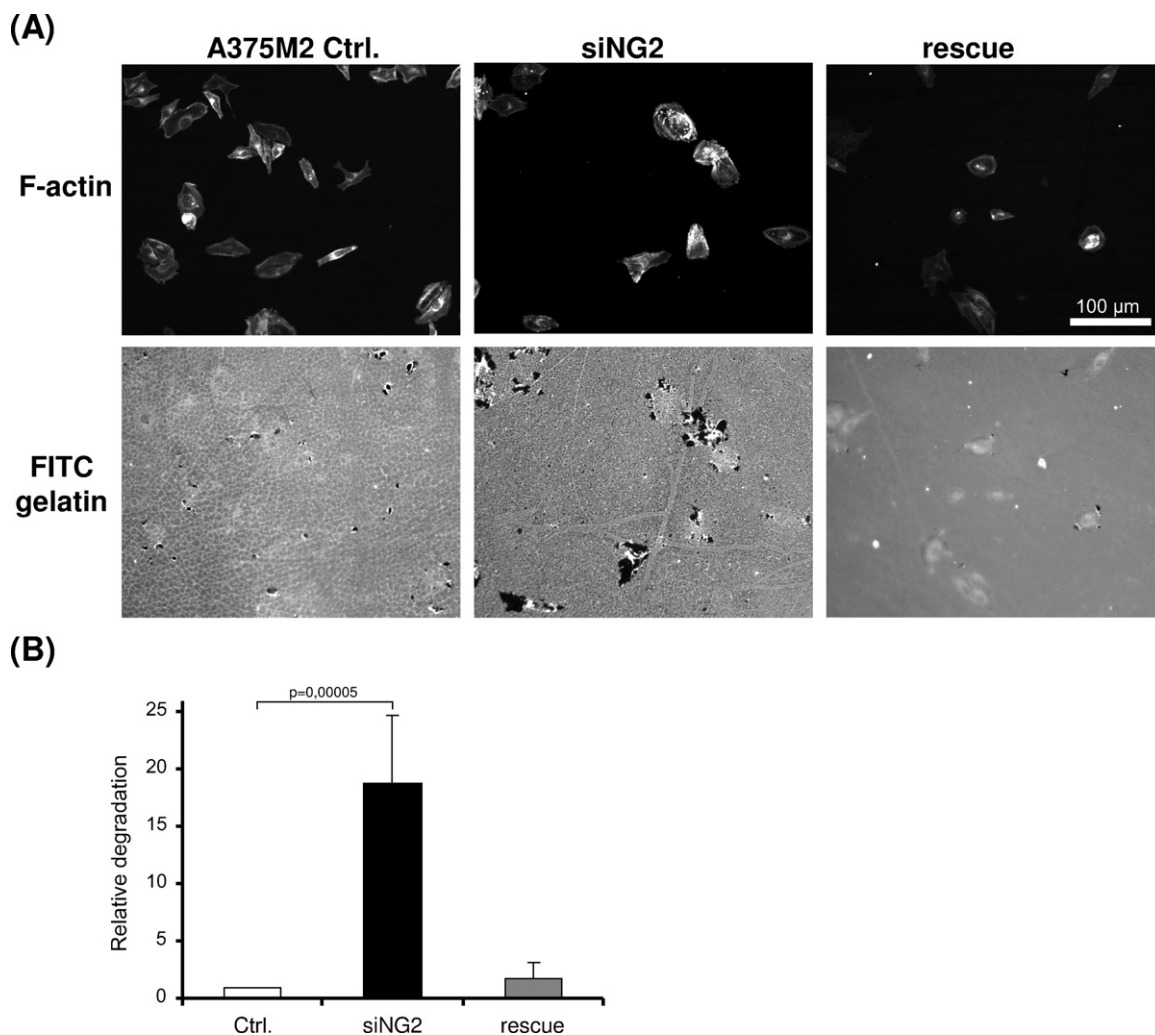


Fig. 5. Effect of NG2 on matrix-degrading activity in A375M2 melanoma cells. (A) Cells were plated on fluorescent gelatin-coated coverslips and subjected to gelatin degradation assay as described in section "Materials and methods". Representative fields were documented by photomicroscopy. Left panel: A375M2 cells; medium panel: A375M2 cells treated with NG2-specific siRNA; right panel: A375M2 cells treated with NG2-specific siRNA and rat NG2 cDNA (rescue). (B) The quantification of matrix-degrading activity was performed as described in section "Materials and methods". Histogram bars represent mean relative degradation obtained from 3 independent experiments and normalized to that of untreated A375M2 cells, the error bars represents standard deviations and p values indicate statistical significances.

We analyzed the potential role of NG2 in amoeboid morphology and invasiveness using two relevant independent systems – rat sarcoma K2 and A3 cells, and human melanoma A375M2 cells. In the highly metastatic amoeboid cell lines, A3 and A375M2, siRNA-mediated down-regulation of NG2 induced an amoeboid-mesenchymal transition, associated with decreased invasiveness in 3D collagen and inactivation of Rho-GTPase. Conversely, the expression of NG2 in mesenchymal sarcoma K2 cells, as well as in A375M2 cells, resulted in an enhanced amoeboid phenotype associated with increased invasiveness and elevated Rho-GTP levels.

Many different signaling mechanisms have been proposed through which NG2 could contribute to malignant transformation (e.g. cell proliferation, cell motility and cell survival) and subsequently promote tumor formation and metastasis (reviewed in Wang et al., 2010). Remarkably, chondroitin sulfate proteoglycans (CSPG) were found to activate Rho/ROCK signaling in processes inhibiting neurite outgrowth (Monnier et al., 2003), which recalls the morphological changes of cells undergoing amoeboid-mesenchymal transition; in fact in both cases, the initially round-shaped cells develop long cellular protrusions. Chondroitin sulfate glycoproteins inhibit neurite outgrowth, an

effect that can be reversed by either Rho or ROCK inhibitors (Monnier et al., 2003). It has also been shown that antibodies against NG2 block its inhibitory effects on neurite growth (Schnell and Schwab, 1990). Taken together, these observations suggest that NG2 inhibits neurite outgrowth through the Rho/ROCK pathway.

An important question is how NG2 could activate Rho/ROCK signaling in the processes of neurite outgrowth inhibition and promotion of amoeboid invasiveness. NG2-mediated intracellular signaling was found to be mainly dependent on the C-terminal half of the cytoplasmic domain. Specifically, MUPP1 protein was identified as an adaptor interacting with PDZ binding motif in the NG2 cytoplasmic domain (Barritt et al., 2000). MUPP1 is a multivalent scaffold, which interacts with the Rho-GEF Syx (Ernkqvist et al., 2009). This interaction subsequently leads to the localized activation of Rho at the leading edge in migrating endothelial cells (Ernkqvist et al., 2009). Indeed, the spatial control of Rho activity was identified as a critical characteristic of amoeboid invasiveness (Wyckoff et al., 2006). Notably, another interacting partner of MUPP1, ezrin, was also found to be essential for effective amoeboid invasion (Sahai and Marshall, 2003).

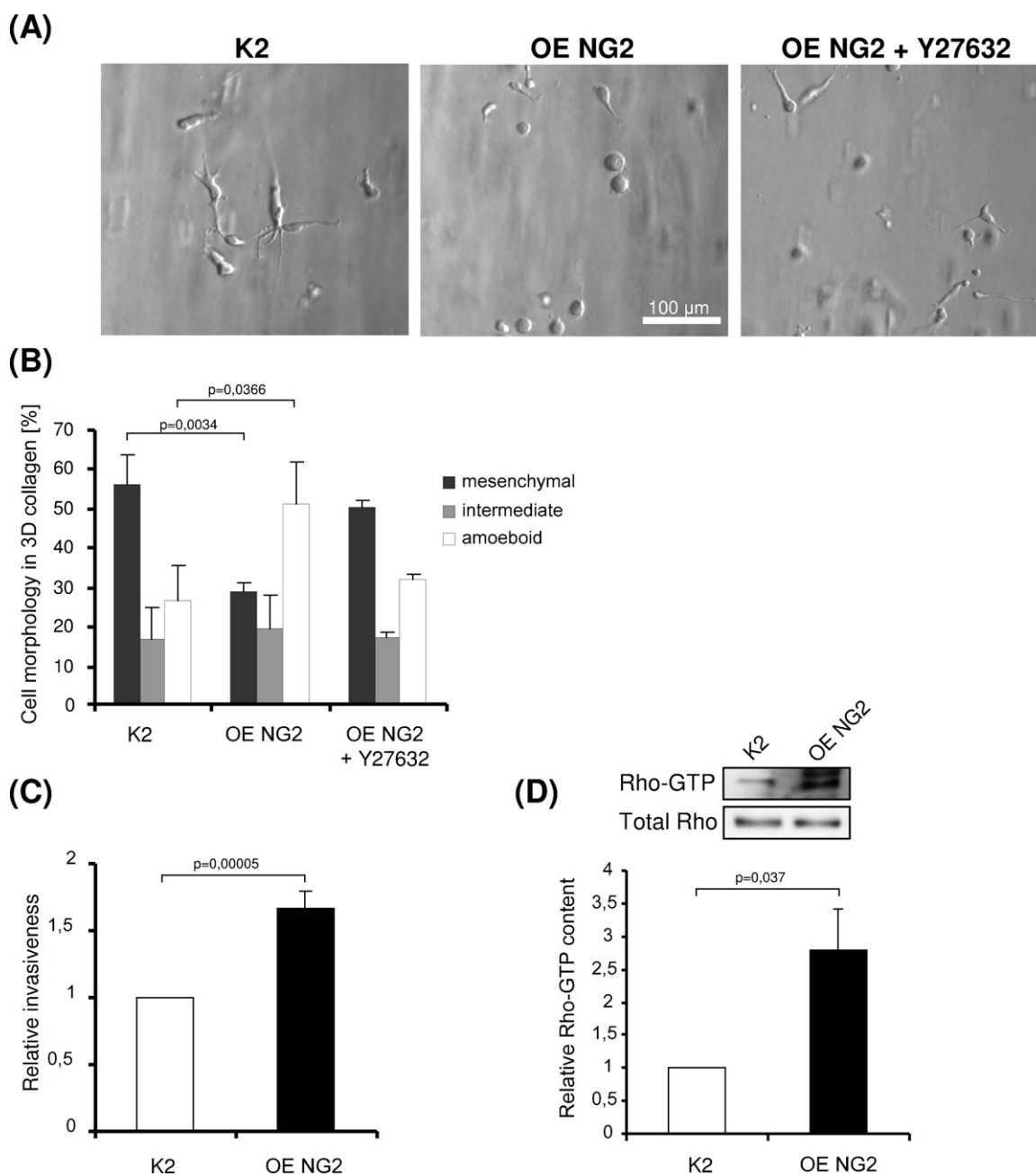


Fig. 6. Effect of NG2 expression in K2 sarcoma cells. (A) Cells were grown in 3D collagen and after 24 h cell morphology was analyzed and documented using photomicroscopy. Left panel: K2 cells; medium panel: K2 cells overexpressing NG2; right panel: K2 cells overexpressing NG2 treated with 10 μ M Y27632. (B) Quantitative analysis of cell morphology. Cells were grown in 3D collagen and after 24 h cell morphology was analyzed using photomicroscopy and classified on the basis of the elongation index as described in section “Materials and methods”. (C) 3D collagen invasion assay. Cells were seeded on top of a collagen gel and their invasion was scored as described in section “Materials and methods”. Bars represent the mean invasion depth, normalized to that of untreated K2 cells. (D) Rho-GTP analysis. Cell lysates of each cell variant were prepared, and total GTP-bound Rho was enriched by absorbing cell lysates to GST-RBD beads and measured by Western blotting using pan-Rho antibody. Densitometric ratios of total Rho and Rho-GTP signal were determined and normalized to that of untreated K2 cells. The error bars represents standard deviations and p values indicate statistical significances. Representative immunoblots of GTP-loaded (upper panel) and total Rho (lower panel) are shown above the graph.

The amoeboid-mesenchymal transition in A375M2 cells with down-regulated NG2 was associated with elevated ECM-degrading ability, although this increase was not sufficient to compensate for the decreased invasive capability caused by down-regulated Rho/ROCK signaling. Conversely, in K2 cells over-expressing NG2, ECM-degrading ability is greatly reduced. The inhibitory effects of NG2 on invadopodia formation and neurite outgrowth, both mediated by Rho/ROCK signaling, suggests that very similar molecular

mechanisms may be responsible for the suppression of invasive protrusions in various biological settings.

Based on the evidence described above, we expect that the upregulation of Rho/ROCK signaling, which leads to effective amoeboid invasiveness, might be one of the mechanisms through which NG2 could contribute to tumor cell invasion and metastasis. Furthermore, NG2 could mediate integrin-independent adhesion.

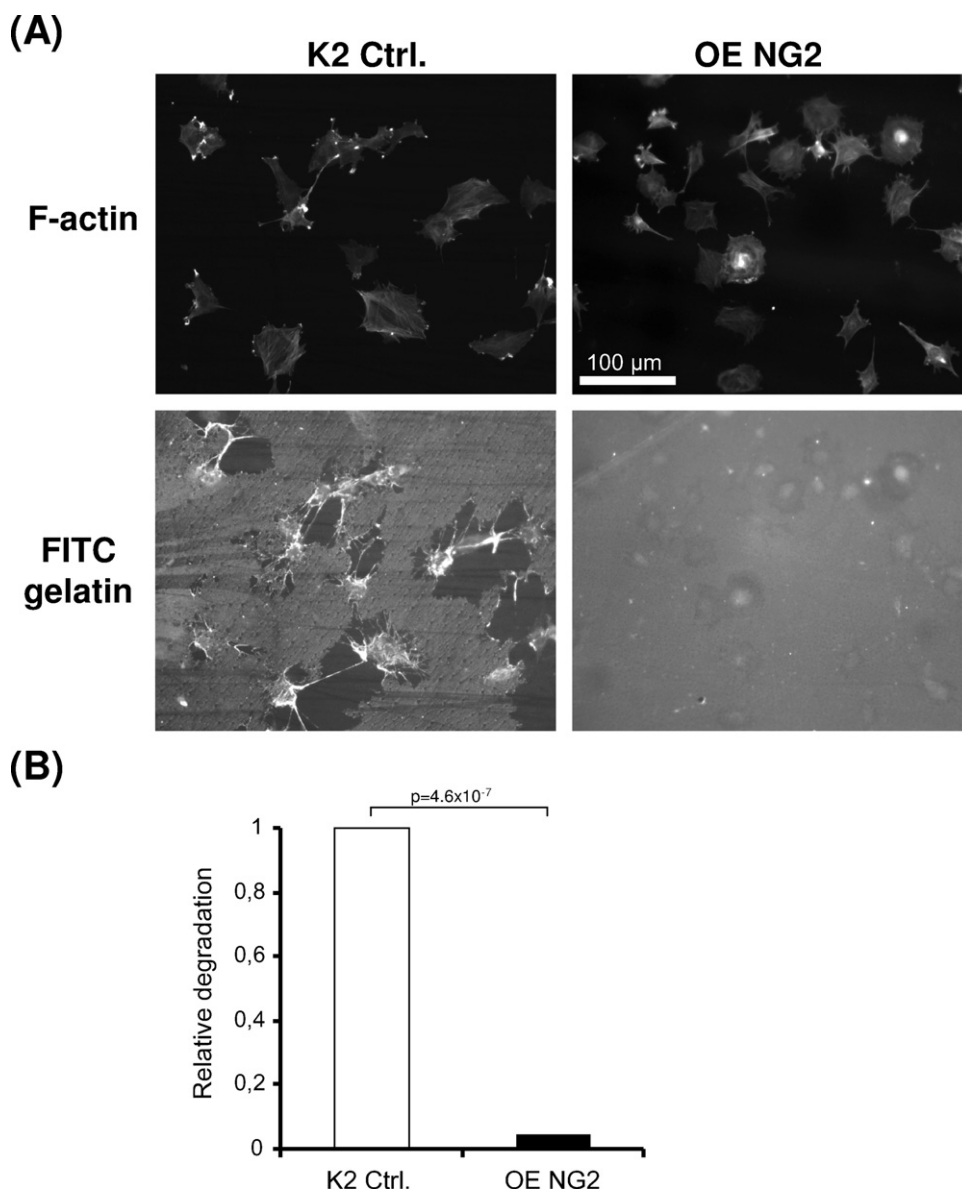


Fig. 7. Effect of NG2 on matrix-degrading activity in K2 sarcoma cells. (A) Cells were plated on fluorescent gelatin-coated coverslips and subjected to gelatin degradation assay as described in section “Materials and methods”. Representative fields were documented by photomicroscopy. Left panel: K2 cells; right panel: K2 cells overexpressing rat NG2 cDNA. (B) The quantification of matrix-degrading activity was performed as described in section “Materials and methods”. Bars represent mean relative degradation obtained from 3 independent experiments and normalized to that of untreated K2 cells, the error bars represents standard deviations and p values indicate statistical significances.

Acknowledgements

We thank Prof. W.B. Stallcup for NG2 cDNA construct, Dr. Francesca Attanasio for expert assistance with gelatin degradation assays, Dr. Jan Svoboda for helping with FACS analysis, Dr. Daniel Zicha for sharing mRNA expression data and Marie Charvátová for excellent technical assistance. This work was supported by Grant Agency of Charles University grant 396611, Czech Ministry of Education, Youth and Sport grant MSM0021620858 and League Against Cancer, Prague and by awards from the Italian Association for Cancer Research (AIRC) and the European Union’s Seventh Framework Programme (grant agreement no. 237946) to RB.

Appendix A. Supplementary data

Supplementary data associated with this article can be found, in the online version, at <http://dx.doi.org/10.1016/j.ejcb.2012.05.001>.

References

- Ayala, I., Baldassarre, M., Giacchetti, G., Caldieri, G., Tetè, S., Luini, A., Buccione, R., 2008. Multiple regulatory inputs converge on cortactin to control invadopodia biogenesis and extracellular matrix degradation. *J. Cell Sci.* 121, 369–378.
- Baldassarre, M., Pompeo, A., Beznoussenko, G., Castaldi, C., Cortellino, S., McNiven, M.A., Luini, A., Buccione, R., 2003. Dynamin participates in focal extracellular matrix degradation by invasive cells. *Mol. Biol. Cell* 14, 1074–1084.
- Barritt, D.S., Pearn, M.T., Zisch, A.H., Lee, S.S., Javier, R.T., Pasquale, E.B., Stallcup, W.B., 2000. The multi-PDZ domain protein MUPP1 is a cytoplasmic ligand for the membrane-spanning proteoglycan NG2. *J. Cell. Biochem.* 79, 213–224.
- Behm, F.G., Smith, F.O., Raimondi, S.C., Pui, C.H., Bernstein, I.D., 1996. Human homologue of the rat chondroitin sulfate proteoglycan, NG2, detected by monoclonal antibody 7.1, identifies childhood acute lymphoblastic leukemias with t(4;11)(q21;q23) or t(11;19)(q23;p13) and MLL gene rearrangements. *Blood* 87, 1134–1139.
- Benassi, M.S., Pazzaglia, L., Chiechi, A., Alberghini, M., Conti, A., Cattaruzza, S., Wassermann, B., Picci, P., Perris, R., 2009. NG2 expression predicts the metastasis formation in soft-tissue sarcoma patients. *J. Orthop. Res.* 27, 135–140.
- Buccione, R., Baldassarre, M., Trapani, V., Catalano, C., Pompeo, A., Brancaccio, A., Giavazzi, R., Luini, A., Corda, D., 2005. Glycerophosphoinositols inhibit the ability of tumour cells to invade the extracellular matrix. *Eur. J. Cancer* 41, 470–476.

- Burg, M.A., Tillet, E., Timpl, R., Stallcup, W.B., 1996. Binding of the NG2 proteoglycan to type VI collagen and other extracellular matrix molecules. *J. Biol. Chem.* 271, 26110–26116.
- Burg, M.A., Grako, K.A., Stallcup, W.B., 1998. Expression of the NG2 proteoglycan enhances the growth and metastatic properties of melanoma cells. *J. Cell. Physiol.* 177, 299–312.
- Caldieri, G., Ayala, I., Attanasio, F., Buccione, R., 2009. Cell and molecular biology of invadopodia. *Int. Rev. Cell Mol. Biol.* 275, 1–34.
- Cavanna, T., Pokorná, E., Veselý, P., Gray, C., Zicha, D., 2007. Evidence for protein 4.1B acting as a metastasis suppressor. *J. Cell Sci.* 120, 606–616.
- Chekenya, M., Rooprai, H.K., Davies, D., Levine, J.M., Butt, A.M., Pilkington, G.J., 1999. The NG2 chondroitin sulfate proteoglycan: role in malignant progression of human brain tumours. *Int. J. Dev. Neurosci.* 17, 421–435.
- Ernkqvist, M., Luna Persson, N., Audebert, S., Lecine, P., Sinha, I., Liu, M., Schlueter, M., Horowitz, A., Aase, K., Weide, T., Borg, J.P., Majumdar, A., Holmgren, L., 2009. The Amot/Patj/Syx signaling complex spatially controls RhoA GTPase activity in migrating endothelial cells. *Blood* 113, 244–253.
- Friedl, P., 2004. Prespecification and plasticity: shifting mechanisms of cell migration. *Curr. Opin. Cell Biol.* 16, 14–23.
- Janostiak, R., Tolde, O., Bruhová, Z., Novotný, M., Hanks, S.K., Rosel, D., Brábek, J., 2011. Tyrosine phosphorylation within the SH3 domain regulates CAS subcellular localization, cell migration, and invasiveness. *Mol. Biol. Cell* 22, 4256–4267.
- Lämmermann, T., Sixt, M., 2009. Mechanical modes of 'amoeboid' cell migration. *Curr. Opin. Cell Biol.* 21, 636–644.
- Monnier, P.P., Sierra, A., Schwab, J.M., Henke-Fahle, S., Mueller, B.K., 2003. The Rho/ROCK pathway mediates neurite growth-inhibitory activity associated with the chondroitin sulfate proteoglycans of the CNS glial scar. *Mol. Cell. Neurosci.* 22, 319–330.
- Nishiyama, A., Dahlin, K.J., Prince, J.T., Johnstone, S.R., Stallcup, W.B., 1991. The primary structure of NG2, a novel membrane-spanning proteoglycan. *J. Cell Biol.* 114, 359–371.
- Panková, K., Rosel, D., Novotný, M., Brábek, J., 2010. The molecular mechanisms of transition between mesenchymal and amoeboid invasiveness in tumor cells. *Cell. Mol. Life Sci.* 67, 63–71.
- Pinner, S., Sahai, E., 2008. PDK1 regulates cancer cell motility by antagonising inhibition of ROCK1 by RhoE. *Nat. Cell Biol.* 10, 127–137.
- Rosel, D., Brábek, J., Tolde, O., Mierke, C.T., Zitterbart, D.P., Raupach, C., Bicanová, K., Kollmannsberger, P., Panková, D., Veselý, P., Folk, P., Fabry, B., 2008. Up-regulation of Rho/ROCK signaling in sarcoma cells drives invasion and increased generation of protrusive forces. *Mol. Cancer Res.* 6, 1410–1420.
- Sahai, E., Marshall, C.J., 2003. Differing modes of tumour cell invasion have distinct requirements for Rho/ROCK signalling and extracellular proteolysis. *Nat. Cell Biol.* 5, 711–719.
- Sanz-Moreno, V., Gadea, G., Ahn, J., Paterson, H., Marra, P., Pinner, S., Sahai, E., Marshall, C.J., 2008. Rac activation and inactivation control plasticity of tumor cell movement. *Cell* 135, 510–523.
- Schnell, L., Schwab, M.E., 1990. Axonal regeneration in the rat spinal cord produced by an antibody against myelin-associated neurite growth inhibitors. *Nature* 343, 269–272.
- Smith, F.O., Rauch, C., Williams, D.E., March, C.J., Arthur, D., Hilden, J., Lampkin, B.C., Buckley, J.D., Buckley, C.V., Woods, W.G., Dinndorf, P.A., Sorensen, P., Kersey, J., Hammond, D., Bernstein, I.D., 1996. The human homologue of rat NG2, a chondroitin sulfate proteoglycan, is not expressed on the cell surface of normal hematopoietic cells but is expressed by acute myeloid leukemia blasts from poor-prognosis patients with abnormalities of chromosome band 11q23. *Blood* 87, 1123–1133.
- Stallcup, W.B., Dahlin, K., Healy, P., 1990. Interaction of the NG2 chondroitin sulfate proteoglycan with type VI collagen. *J. Cell Biol.* 111, 3177–3188.
- Stallcup, W.B., Huang, F.J., 2008. A role for the NG2 proteoglycan in glioma progression. *Cell Adh. Migr.* 2, 192–201.
- Tillet, E., Ruggiero, F., Nishiyama, A., Stallcup, W.B., 1997. The membrane-spanning proteoglycan NG2 binds to collagens V and VI through the central nonglobular domain of its core protein. *J. Biol. Chem.* 272, 769–776.
- Tillet, E., Gentil, B., Garrone, R., Stallcup, W.B., 2002. NG2 proteoglycan mediates beta1 integrin-independent cell adhesion and spreading on collagen VI. *J. Cell. Biochem.* 86, 726–736.
- Tolde, O., Rosel, D., Veselý, P., Folk, P., Brábek, J., 2010. The structure of invadopodia in a complex 3D environment. *Eur. J. Cell Biol.* 89, 674–680.
- Wang, X., Wang, Y., Yu, L., Sakakura, K., Visus, C., Schwab, J.H., Ferrone, C.R., Favoino, E., Koya, Y., Campoli, M.R., McCarthy, J.B., DeLeo, A.B., Ferrone, S., 2010. CSPG4 in cancer: multiple roles. *Curr. Mol. Med.* 10, 419–429.
- Wolf, K., Mazo, I., Leung, H., Engelke, K., von Andrian, U.H., Deryugina, E.I., Stroganov, A.Y., Bröcker, E.B., Friedl, P., 2003. Compensation mechanism in tumor cell migration: mesenchymal-amoeboid transition after blocking of pericellular proteolysis. *J. Cell Biol.* 160, 267–277.
- Wyckoff, J.B., Pinner, S.E., Gschmeissner, S., Condeelis, J.S., Sahai, E., 2006. ROCK- and myosin-dependent matrix deformation enables protease-independent tumor cell invasion in vivo. *Curr. Biol.* 16, 1515–1523.